Available online at www.sciencedirect.com
ScienceDirect
Journal of Nuclear Materials 363–365 (2007) 498–504
journal of nuclear materials
www.elsevier.com/locate/jnucmat

# Role of recycling in JET trace tritium transport experiments

D.L. Hillis [a,*], J. Hogan [a], K.-D. Zastrow [b], V. Parail [b], D. Coster [c], D. Reiter [d], S. Brezinsek [d], A. Pospieszczyk [d], M. Stamp [b], W. Fundamenski [b], D.C. McDonald [b], JET EFDA Contributors [1]

[a] *Oak Ridge National Laboratory, Oak Ridge, TN 37831, USA*
[b] *EURATOM/UKAEA Fusion Association, Culham Science Centre, Abingdon OX14 3DB, UK*
[c] *EURATOM/IPP-Garching Fusion Association, Max Planck Institut, Garching, Germany*
[d] *EURATOM/FZ-Juelich, Juelich, Germany*

**Abstract**

JET experiments with transient puffed injection of low tritium levels were carried out with the goal of using measured time- and space-dependent neutron emission to determine the scaling of particle transport in the core for ITB, ELMy H-mode and hybrid scenarios. Several attempts to find core $\tau_p$ scaling based on the same dataset have reached contradictory conclusions: core particle diffusivity inversely proportional to density, scaling proportional to density, and scaling independent of collisionality (density independence). The analyses have also varied the assumed boundary conditions. In all three cases, ELM-averaged transport was analyzed. To see what can be learned about resolution of such differences through possible systematic SOL effects on particle transport scaling, using the available edge/SOL data for these core particle transport experiments, we analyze representative cases from the JET trace T experimental database. The pulses considered cover a range in average core electron density, with approximately constant tritium puffing rates. The study is motivated by the realization that, although these experiments were not designed for such a purpose, similar future 'trace T' experiments could better characterize the SOL, and thus its influence of on particle transport in the edge/pedestal region ($0.8 < \rho < 1$) since important elements of the tritium pathway are measured: the external $T_2$ gas puff rate ($\Gamma_{\mathrm{puff}}^{\mathrm{max}}$), and, from the neutron analysis, the influx to the plasma core region at $\rho = 0.8$ ($\Gamma_{\mathrm{T+}}^{\mathrm{in,max}}$) and the efflux from the core ($\Gamma_{\mathrm{T+}}^{\mathrm{out,max}}$). Systematic effects on edge/pedestal particle transport scaling in puffing experiments are found to depend on the status of saturation in the near-inlet region, on the details of ELM-induced particle expulsion from both core and SOL, and on the degree of near-wall T enrichment.


## 1. Introduction

JET experiments with transient puffed injection of low tritium levels (<1%) were carried out with the goal of using measured time- and space-dependent neutron emission to determine the $\rho^*$, $\nu^*$ and $\beta$ scaling of particle transport in the core

* Corresponding author. Tel.: +1 865 576 3739; fax: +1 865 574 1191.
*E-mail address:* hillisdl@ornl.gov (D.L. Hillis).
[1] See the Appendix of J. Pamela et al., Fusion Energy 2004 (Proc. 20th Int. Conf. Vilamoura, 2004) IAEA, Vienna (2004).

0022-3115/$ - see front matter © 2007 Elsevier B.V. All rights reserved.
doi:10.1016/j.jnucmat.2006.12.069

(normalized radius $\rho < 0.8$) for ITB, ELMy H-mode and hybrid scenario [1]. Although the diagnostics were well suited to this task, several attempts to find core $\tau_p$ scaling based on the same dataset have reached contradictory conclusions. For example, a scaling of core particle diffusivity inversely proportional to density was found in [2] using an interpretive–predictive approach, a scaling proportional to density in [3] using predictive modeling, and a scaling independent of collisionality (density independence) in [1] by fitting the neutron emission data. The analyses cited have also varied the assumed boundary conditions. In [1], a three reservoir model was used for the region exterior to the core, with model parameters varied as needed to fit the time behavior of the outermost neutron channel. In [2], the boundary value of the tritium density was assumed small enough not to influence the core simulations, with a value of core tritium recycling from 3% to 7% of the total deuterium and tritium flux. Finally, in [3], it was assumed that $0 < R_T^{core} < 1$. The core tritium recycling coefficient $R_T^{core}$ is defined as the ratio of T influx to the core to the T efflux from the core. In all three cases, ELM-averaged transport was analyzed.

To see what can be learned about resolution of such differences through possible systematic SOL effects on particle transport scaling, using the available edge/SOL data for these core particle transport experiments, we analyze representative cases from the JET trace T experimental database, with a range of parameters as given in Table 1. Both puffing and neutral beam injection were used to inject tritium in the trace T campaign, and both neutral beam and RF heating were used. Here we analyze only tritium puffing cases, with neutral beam heating only. The pulses considered cover a range in average core electron density, with approximately constant tritium puffing rates. These cases were used to represent a density scan in [2], but plasma current, magnetic field and shape vary. There are also important systematic differences in ELM behavior for the cases in Table 1, as shown in Fig. 1. The study is motivated by the realization that, although these experiments were not designed for such a purpose, similar future 'trace T' experiments could better characterize the SOL, and thus its influence on particle transport in the edge/pedestal region ($0.8 < \rho < 1$) since important elements of the tritium pathway are measured: the external $T_2$ gas puff rate ($\Gamma_{puff}^{max}$), and, from the neutron analysis, the influx to the plasma core region at $\rho = 0.8$ ($\Gamma_{T+}^{in,max}$) and the efflux from the core ($\Gamma_{T+}^{out,max}$).

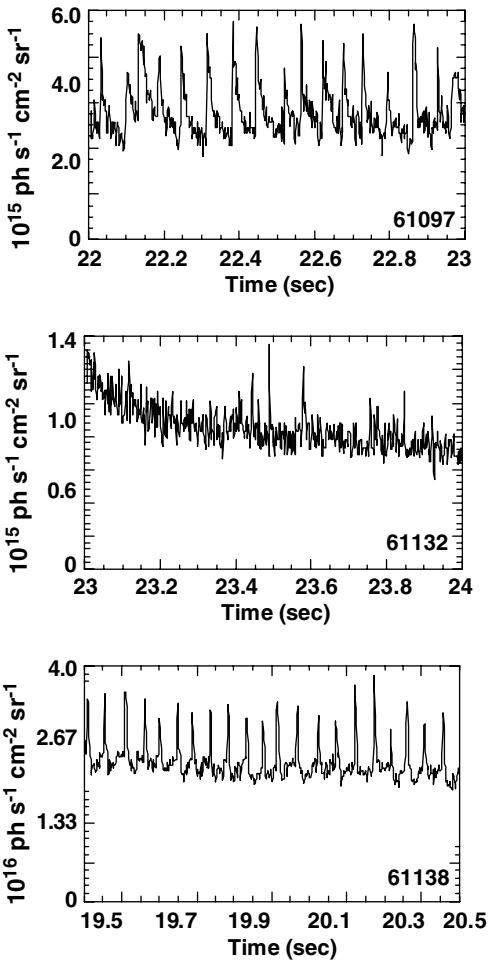


Fig. 1. Comparison of ELM activity for the cases considered in the analysis (parameters in Table 1).

Table 1
Parameters for analyzed T puffing cases

| Shot | $\langle n_e \rangle$ ($10^{19}$ m$^{-3}$) | $\Gamma_{puff}^{max}$ ($10^{22}$ pt/s) | $\Gamma_{T+}^{in,max}$ ($10^{19}$ pt/m$^2$/s) | $\Gamma_{T+}^{out,max}$ ($10^{19}$ pt/m$^2$/s) | $N_{core}$ ($10^{19}$ pt) | $B_T$ (T) | $I_p$ (MA) | $P_{NB}$ (MW) |
|---|---|---|---|---|---|---|---|---|
| 61132 | 2.4 | 1.1 | 3.6 | 2.2 | 16.0 | 1.9 | 2.35 | 2.3 |
| 61097 | 5.0 | 1.22 | 3.3 | 2.8 | 8.0 | 1.65 | 2.0 | 7.6 |
| 61138 | 9.5 | 1.12 | 2.7 | 2.4 | 4.6 | 2.25 | 2.5 | 13.6 |

Such SOL-based analysis of trace tritium injection would also have obvious value in identifying the pathways of injected tritium, its fueling efficiency, and its eventual retention.

We analyze the tritium pathway from injection to the core boundary, with attention to the gas inlet region, in Section 2, and the systematic effects of wall saturation and ELMs in Sections 3 and 4, respectively. Conclusions are presented in Section 5.

## 2. Tritium pathways

The sensitivity of previous core transport analysis to tritium recycling assumptions suggests that we first obtain an overall view of this process.

### 2.1. T pathway from injection to core plasma

Tritium was injected in these experiments from a large port on the outboard mid-plane in JET (Gas Introduction Module 15 – GIM15). The injected tritium amount is determined by measuring pressure drop in a chamber connected to a valve which is located ~160 cm outside the outer scrape-off layer. If parasitic plasma exists in this port, there is a chance for significant attenuation of the injected T and deposition in the port before entering the SOL. After entering the SOL the injected $T_2$ undergoes ionization, dissociation and charge exchange processes before a fraction reaches the separatrix. From the separatrix there is a preferential loss from the pedestal region due to ELMs before the injected $T^+$ ions reach the outermost core radius where neutron emission statistics are satisfactory, at normalized radius $\rho = 0.82$.

To establish the overall tritium environment for the analyzed cases, Fig. 2(a) illustrates the sequence of all tritium puffing shots in the JET trace T campaign prior to the latest pulse analyzed here in. Fig. 2(a) shows both the instantaneous tritium puffing rate (the peak rate is $\sim 10^{22}\ s^{-1}$), and the accumulated T injected by puffing, and serves to locate the analyzed cases within this time history. For example, it should be noted that there was no T puffing for the 30 pulses just preceding the first shot considered (61097).

The measured core T content, from neutron analysis, and the injected T values are shown in Fig. 2(b). The measured core T content is <10% of the injected T values, for the cases studied, so core T recycling occurs in a background of a much larger T recycling flux in the SOL and wall region. Thus, it

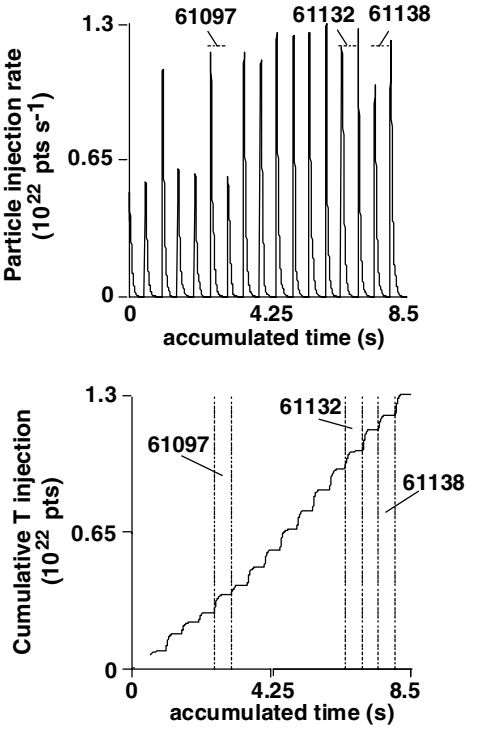


Fig. 2(a). Tritium puffing rate (top) and accumulated puffed tritium for all tritium cases preceding those analyzed (parameters in Table 1).

is not clear *a priori* that the value of $R_T^{core}$ should be small (e.g., <1). Further, the non-penetrating component of the injected flux could produce a localized cool, dense region near the inlet, as was observed on Textor-94 [4]. It should be noted that even though the trace T experiments provide a T level which is <1% of the D density, the locally injected T from the JET gas valve provides this level for a 30-times greater plasma volume in JET, as compared with Textor-94, and with a smaller power density. So the possibility of a localized cool, dense region near the inlet, while not proven, remains a possibility.

To characterize the external tritium pathway we used an idealized multi-species simulation with the solps code (coupled b2 and Eirene) using an Eirene model developed by Reiter and Coster [5], to calculate the distribution of D, T, $D_2$, DT, $T_2$ in the near-inlet region. Fig. 3 shows the resulting spatial distribution of T fluxes and energies to the wall in a near-inlet region (localized 20 cm poloidally around the gas inlet) for the shots in the table. Two cases are considered for each shot, assuming the total net power crossing the separatrix $P_{sptrx} = 0.5$ and $0.75P_{NB}$. An elevated flux of low energy atoms and molecules is found in the central

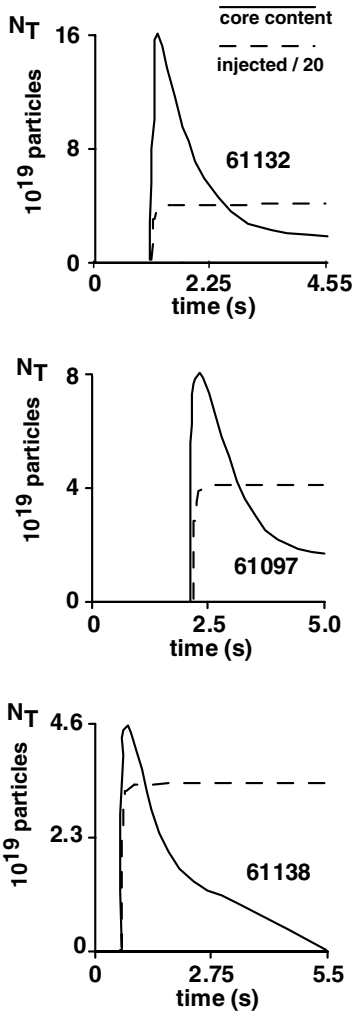


Fig. 2(b). Time dependence of the measured T influx rate and core T content for the cases analyzed.

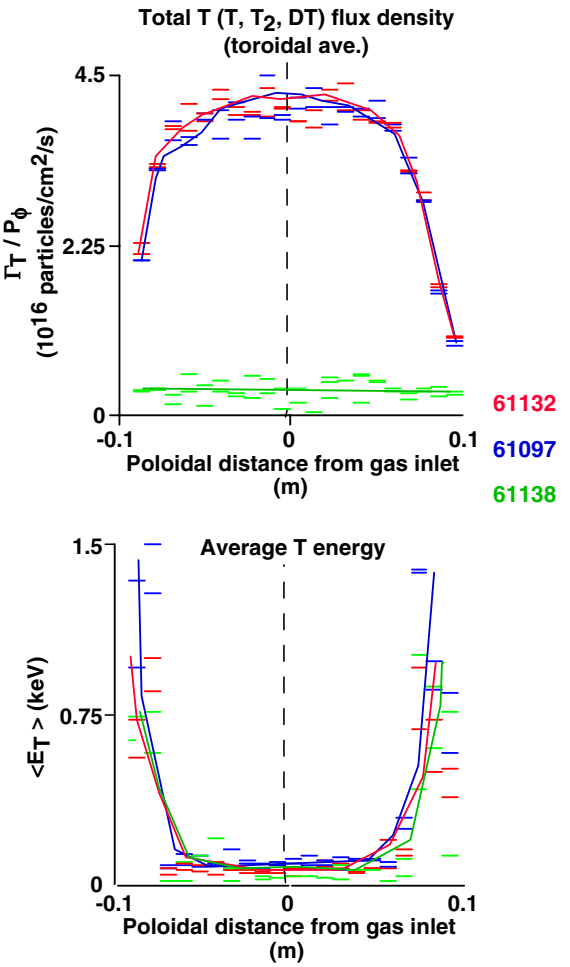


Fig. 3. Local T fluxes (top) and energies (bottom) near the puffing location for conditions of the cases analyzed. Two cases are presented for each shot, assuming net power to the SOL is 0.5 and $0.75 \times P_{\text{input}}$. Lines are drawn with the Monte Carlo data to guide the eye.

port region, and is distinguished from the low flux, high energy values for core CX particles in the wings. Note: these particle flux values are toroidally averaged, although the calculation assumes an idealized point T source and is three-dimensional. Fig. 3(a) also shows a significant reduction in the T flux to the wall for the highest density case (61138), reflecting reduced mean free path (trapping in the SOL with flow to the divertor) and diminution of Franck–Condon neutral production. This is consistent with the decreased core T content (table) for pulse 61138. Thus, systematic density-dependent variations in wall saturation can be expected to play a role in edge/pedestal particle transport scaling.

The core boundary condition for tritium depends on the local T enrichment in the pedestal region. To illustrate the relation between SOL values and the boundary conditions which are used in core transport analysis, Fig. 4(a) and (b) shows solps results for the $T^+$ concentrations in the near-wall region and at the separatrix for the cases considered, as a function of the flux coordinate on the outboard (low-field) side. Strong local near-wall T enrichment is seen, decreasing toward the edge/pedestal and a systematic reduction on the separatrix tritium concentration as density is increased, with the near-wall concentration remaining constant, reflecting the constant tritium puffing rate. The dashed line indicates the inlet position. Comparison with the available partial ELM-averaged divertor langmuir probe data is shown only to indicate that the solutions are in

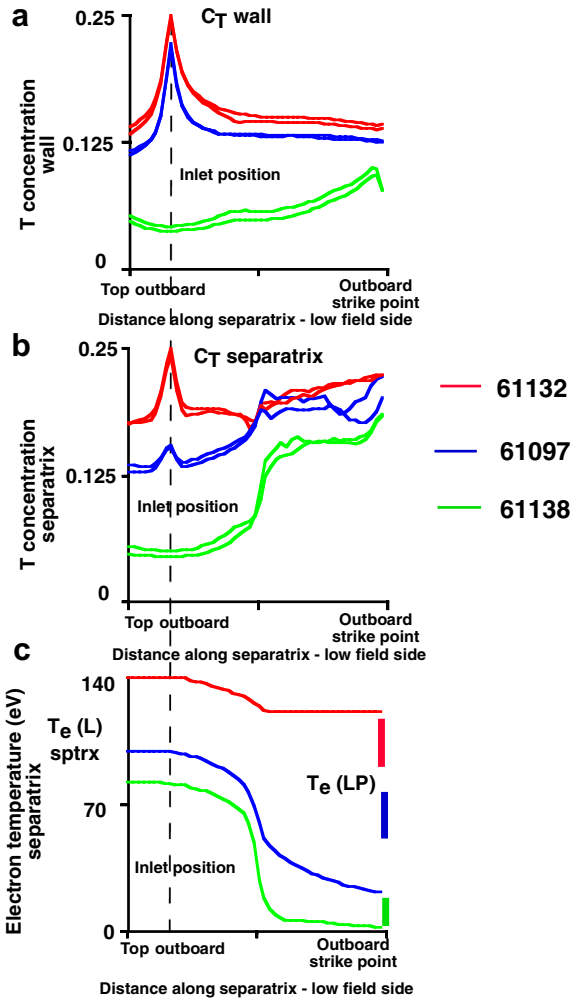


Fig. 4. Variation of near-wall and separatrix parameters on the low-field side, assuming $P_{SOL} = 0.5$, $0.75P_{in}$: (a) tritium ion concentration near the wall, (b) tritium ion concentration at the separatrix and (c) variation in electron temperature compared with available langmuir probe data at the outboard strike point for the three cases considered, assuming $P_{SOL} = 0.5P_{in}$.

scale for the density range considered (Fig. 4(c)). The local concentration of tritium in the wall-pedestal region is considerably higher than the overall core plasma average. However this range of local values is consistent with those found from molecular spectroscopic observations viewing GIM15, which were made under similar conditions for H injection into D plasmas [6].

## 3. Systematic effects on scaling: wall saturation

The value of $R_T^{core}$ which is needed for core transport analysis is related to $R_T^{wall}$ (the ratio of T fluxes entering and leaving the wall). The plasma-facing surfaces near the gas introduction module used for tritium puffing are a mixture of CFC and graphite, materials which are well known to have a large capacity to store implanted hydrogen. A number of models have been proposed for hydrogen inventory dynamics and several have been incorporated in the 1D, time-dependent WDIFFUSE code [7]. WDIFFUSE treats deuterium and tritium and calculates the evolution of $D_2$, D–T and $T_2$ in the surface, following the space- and time-dependent evolution of both trapped (t) and solute (s) hydrogenic species under the interaction of deuterium and tritium implanted fluxes. In the implantation zone the model equations for the solute concentrations are

$$\frac{\partial c_s^D}{\partial t} = -k_0 (c_s^D)^2 - k_0 c_s^D c_s^T - \frac{\partial c_t^D}{\partial t} + \Sigma^D + D_D \frac{\partial^2}{\partial x^2} c_s^D, \tag{1}$$

and

$$\frac{\partial c_s^T}{\partial t} = -k_0 (c_s^T)^2 - k_0 c_s^D c_s^T - \frac{\partial c_t^T}{\partial t} + \Sigma^T + D_T \frac{\partial^2}{\partial x^2} c_s^T. \tag{2}$$

For the trapped concentrations, the equations are

$$\frac{\partial c_t^D}{\partial t} = k_{s,t} c_s^D \left(1 - \frac{(c_t^D + c_t^T)}{c_{t,s}}\right) - k_{t,s} c_t^D - k_d c_t^D (\Sigma^D + \Sigma^T)^{1/2} - \sigma_{dt} c_t^D (\Sigma^D + \Sigma^T), \tag{3}$$

and

$$\frac{\partial c_t^T}{\partial t} = k_{s,t} c_s^T \left(1 - \frac{(c_t^T + c_t^D)}{c_{t,s}}\right) - k_{t,s} c_t^T - k_d c_t^T (\Sigma^D + \Sigma^T)^{1/2} - \sigma_{dt} c_t^T (\Sigma^D + \Sigma^T), \tag{4}$$

where subscripts t and s refer to trapped or solute states, D and T refer to the species (deuterium or tritium), $\Sigma$ is the implantation rate, $c_s^D$ and $c_s^T$ are the solute concentrations for deuterium and tritium, $k_0$ is the recombination coefficient, $k_{t,s}$ is the thermal detrapping coefficient, $k_{s,t}$ is the trapping coefficient, and $k_d$ and $\sigma_{dt}$ are the particle-induced detrapping coefficients.

Values used for the models considered here are given in Table 2. Ehrenberg created a semi-empirical model, extending the model for post-shot T decay in JET Preliminary Tritium Experiments (PTE) to include particle-induced detrapping rates [8]. The empirical coefficients for particle-induced detrapping rates were obtained from analysis of

Table 2
Surface model coefficients used in the WDIFFUSE code

| Model/coefficient | Ehrenberg semi-empirical | Grisolia et al. | Empirical |
|---|---|---|---|
| Recombination: $k_0$ ($cm^3/s$) | $2.5\times10^{-21}$ | $10^{-20}$ | $2.5\times10^{-21}$ |
| Thermal detrapping: $k_{t,s}$ ($s^{-1}$) | 0 | $5\times10^{-2}$ | 0 |
| Trapping: $k_{s,t}$ ($s^{-1}$) | $10^4$ | $10^2$ | $10^4$ |
| Detrapping: $\sigma_{dt}$ ($cm^{-2}$) | 0.0 | $8\times10^{-17}$ | 0 |
| Particle-induced detrapping: $k_d$ ($cm^{3/2}/s^{1/2}$) | $6\times10^{-13}$ | 0 | $6\times10^{-13}$ |
| Particle-induced detrapping $\propto \Phi^{\alpha}$ ($\Phi$ flux); $\alpha$: | 0.5 | 1.0 | 0.5 |
| Diffusivity: deuterium ($cm^2/s$) | $1.0\times10^{-7}$ | $7.5\times10^{-15}$ | $4\times10^{-14}$ |

previous JET tritium puffing experiments during full-scale D–T experiments (DTE). Another successful model for particle-induced desorption has been proposed by Grisolia et al. to fit Tore Supra post-shot decay experiments [9]. Larger values for bulk diffusivity have been determined for CFC components [10] and these values are consistent with prior results of T depth profiling after JET DTE experiments [11] and from preliminary analysis of the current trace tritium experiments discussed here. Thus we also evaluated a hybrid empirical model, with rates as in the Ehrenberg model but using the larger diffusivities, which may be relevant for CFC.

Fig. 5 shows the calculated WDIFFUSE time evolution of the near-inlet $R_T^{wall}$, using the Ehrenberg, Grisolia et al. and 'empirical' models, and the calculated solps fluxes for the chosen pulses. The transient of $R_T^{wall}$ is found to vary systematically with the density for all the models, and to have significant quantitative variation between the models as well. Recall that the effect on core density behavior enters as $\frac{1}{1-R_T^{core}}$. For these values, the calculated T fluxes and energies would produce a saturated near-inlet surface region (local ratio $n_T/n_C > 0.4$) within ~25–100 ms. It should be stressed that the results strongly depend on the assumed prior implantation history and on the assumed distribution of trapped T in the surface before the simulation. Conditions chosen here are based on the data shown in Table 1. As seen in Fig. 2(b), the prior accumulated T puffing injection varies by a factor 3 for the cases considered which influences the starting conditions for recycling calculations.

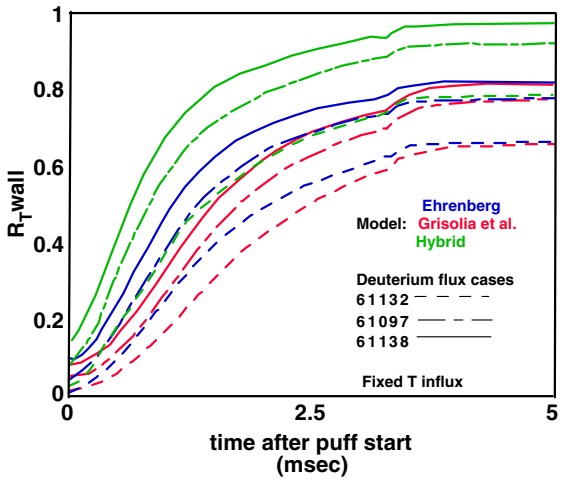


Fig. 5. Wall tritium recycling response during the tritium puff for three wall models: (blue) Ehrenberg semi-empirical, (red) Grisolia et al. (green) hybrid model replacing diffusivity in the Ehrenberg model for higher values appropriate for CFC. Each of the models is evaluated for influx conditions of the shots analyzed.

## 4. Systematic effects on scaling: pedestal/ELMs

The differences in ELM behavior for these cases (as shown in Fig. 1) can also have a systematic effect on particle transport scaling. Calculations have been made with the MIST radial transport code [12] for these shots, to consider ELM-related effects *in isolation from wall recycling effects*. The calculations use an explicit ELM model to replace ELM-averaged values, and find that the turbulent (excess over neo-classical) diffusivities which match the transient in the edge/pedestal region to be reduced by a factor 2–4 for the isolated/compound ELM cases ($0.2/0.6\ m^2\ s^{-1}$ reduced to $0.05/0.2\ m^2\ s^{-1}$, respectively) and by 5-fold for the grassy ELM case ($2.5–0.5\ m^2\ s^{-1}$).

Systematic ELM-related scaling effects on the SOL/pedestal region have been studied using a multi-species (D, T, $D_2$, DT, $T_2$) solps simulation to estimate the degree of variation in wall fluxes during ELMs. Fig. 6 compares the $n_D^+$ and $n_T^+$ evolution in the divertor (top) and in the SOL upstream of the *x*-point. A transient increase in local fluxes by 3-fold is found, which would intensify the model- and density-dependent WDIFFUSE results for $R_T^{core}$ and $R_T^{wall}$. However, development of a quantitative

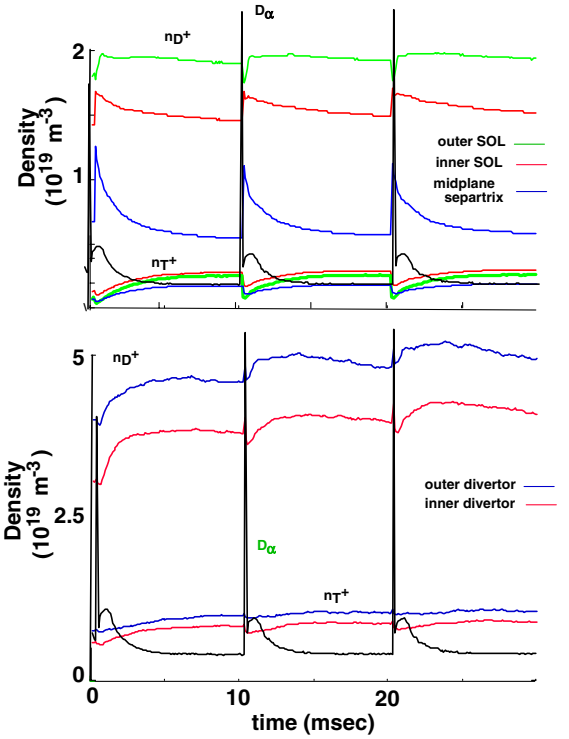


Fig. 6. Solps simulation of the variation of $D^+$ and $T^+$ densities in the SOL during a series of ELMs, for conditions modeling pulse 61097. The simulated $D_\alpha$ behavior is shown to indicate ELM frequency.

model for the details of ELM effects on the pedestal region is under study.

## 5. Conclusions

Systematic effects on edge/pedestal particle transport scaling in puffing experiments depend on the status of saturation in the near-inlet region, on the details of ELM-induced particle expulsion from both core and SOL, and on the degree of near-wall T enrichment. Further progress in quantifying and in clarifying the roles of these processes could be achieved through dedicated experiments on edge/pedestal trace T transport, to complement previous core studies.

## Acknowledgement

ORNL. Supported by US DOE Contract DE-AC05-00OR22725.

## References

[1] K.-D. Zastrow, K.M. Adams, Y. Baranov, et al., Plasma Phys. Contr. Fusion 46 (2004) B255.
[2] I. Voitsekovitch, X. Garbet, D.C. McDonald, et al., Phys. Plasmas 12 (2005) 052508.
[3] P. Belo, V. Parail, et al., in: Proceedings of the 31st EPS Conference on Plasma Physics, London, 2004, p. 1.
[4] B. Unterberg et al., J. Nucl. Mater. 337–339 (2005) 515.
[5] D. Reiter, D. Coster, private communication, 2002.
[6] S. Brezinsek, A. Pospieszczyk, et al., in: Proceedings of the 32nd EPS Conference on Plasma Physics, Tarragona, 2005, p. 2.
[7] D. Hillis et al., Phys. Plasmas 6 (1999) 1985.
[8] J. Ehrenberg, personal communication, 1998.
[9] C. Grisolia, L.D. Horton, J. Ehrenberg, J. Nucl. Mater. 220 (1995) 516.
[10] L.A. Sedano, A. Perujo, C.H. Wu, et al., J. Nucl. Mater. 273 (1999) 295.
[11] R.-D. Penzhorn, N. Bekris, U. Berndt, J.P. Coad, H. Ziegler, W. Nägele, J. Nucl. Mater. 288 (2001) 170.
[12] R.A. Hulse, Fusion Technol. 3 (1982) 259.